Published in Electrochemistry Communications 10 (2008) 1905–1908 -
doi:10.1016/j.elecom.2008.10.010

High Performance Nanostructured IT-SOFC Cathodes Prepared by Novel Chemical Method

Laura Baqué, Alberto Caneiro, Mario S. Moreno, and *Adriana Serquis**

CONICET - Centro Atómico Bariloche, Temadi, Av. Bustillo 9500, Bariloche, 8400 San Carlos de Bariloche, Río Negro, Argentina
*Corresponding author. TE: +54 2944 445288 E-mail address: aserquis@cab.cnea.gov.ar

Keywords: solid oxide fuel cell; cathode materials; mixed conductor; polymeric solution

Abstract

The electrochemical performance of $La_{0.4}Sr_{0.6}Co_{0.8}Fe_{0.2}O_{3-\delta}$ (LSCF) cathodes with different nano/microstructures is compared using the area specific resistance (ASR). Cathodes are prepared using two chemical routes, including a novel method to obtain nanosized LSCF oxide. The results clearly point that the intermediate temperature Solid Oxide Fuel Cells (IT-SOFC) cathode performance strongly depends on microstructure and that ASR can vary more than two orders of magnitude for identical composition and different morphologies, reaching values as low as 0.05 Ωcm^2 at 600˚C and 0.4 Ωcm^2 at 450˚C using the novel chemical route, which are even lower than the best known cathodes for IT-SOFC.

1. Introduction

The employment of new electrolyte materials (like gadolinium doped ceria and lanthanum gallate) allowed the development of intermediate temperature solid oxide fuel cells (IT-SOFC), which represent an alternative to conventional SOFC (with yttria-stabilized zirconia electrolyte) because of its lower operation temperature (500 - 700ºC) and cost [1]. However, cathode overpotential becomes important at these temperatures [2], decreasing the cell performance.
Most of research work focused to enhance cathode performance only deal with chemical composition, although microstructure is also relevant. For instance, nanostructured materials with a high surface area would further improve cathode performance [3-8]. Nevertheless, the high temperatures involved for phase formation of IT-SOFC cathode materials hinder the possible achievements of nanostructures.
In this work, $La_{0.4}Sr_{0.6}Co_{0.8}Fe_{0.2}O_{3-\delta}$ (LSCF) cathodes are prepared using two chemical methods, including a novel one developed from two known chemical routes [9,10] which allows the formation of nanosized LSCF oxide. Then, the electrochemical performance of cathodes with different nano/microstructures is compared using the area specific resistance (ASR), as is standard in this field.

2. Experimental

$La_{0.4}Sr_{0.6}Co_{0.8}Fe_{0.2}O_{3-\delta}$ powder was prepared by two different methods (from now on called Acetate and HMTA). Stoichiometric amounts of $SrCO_3$, La_2O_3, $Fe(CH_3COO)_2$, and $Co(CH_3COO)_2 \cdot 4H_2O$ were dissolved in acetic acid for the Acetate method and in an acetic acid, hexamethylenetetramine (HMTA) and acetylacetone (AcAc) solution for the novel HMTA method. In the latter, organic to inorganic components concentration ratio c_o/c_i was fixed to 3.1, where $c_i = c_{La} + c_{Sr} = c_{Co} + c_{Fe}$ and $c_o = c_{HMTA} = c_{AcAc}$. The obtained mixtures were refluxed at T~ 80 °C and then sufficient amounts of water and hydrogen peroxide were

added to get a clear solution. These solutions were refluxed for one more hour and then were evaporated until transparent gels were formed. These gels were fired at 400°C for 2 hours and then milled in an agate mortar. The obtained powders, as pressed pellets, were sintered at the temperature (T_S) indicated in Table 1 and then ball milled.
Two different inks were prepared for cathode deposition, mixing the powder sintered by each chemical route with ethanol, terpineol, polyvinyl butyral, and polyvinyl pyrridone in same weight percentage for both inks. The used powders were sintered at a temperature slightly below to that corresponding to the phase formation for each method (i.e. T_S = 800°C for Acetate and T_S= 750°C for HMTA methods). The $Ce_{0.9}Gd_{0.1}O_{2-\delta}$ (CGO) electrolyte substrates were prepared by pressing pellets of commercial powder (Praxair) into 12.5 mm diameter discs, 1 mm thick and firing them at 1350 °C during 12 h. Films were deposited onto both sides of rectified CGO substrates by spin coating technique, resulting in a symmetrical cell configuration used for electrochemical measurements [11]. Afterwards, these assemblies were heat treated at the temperature (T_{HT}) indicated in Table 2 for 6 h in air to reach a sufficient adherence between electrodes and electrolyte. To check the reproducibility of the preparation and measurement process, two cathode films were identically prepared for each method.
ASR cathodes values were determined from impedance spectroscopy measurements (EIS) under Ar-O_2 mixture, with oxygen partial pressure corresponding to air, carried out heating from 400 to 700 °C (50ºC steps), and cooling down [5].

3. Results and Discussion

Powders were sintered at the minimum required temperature to obtain a single LSCF phase (determined previously in a high temperature X-ray diffraction, XRD, camera) and at another one slightly below it, as can be seen in Figure 1a where only XRD patterns from samples A900 and H800 correspond to single LSCF phase without presence of non-reacted oxides.
Crystallite sizes were determined from XRD data, analyzing selected LSCF phase reflections by Scherrer formula (see Table 1). Powders sintered at temperatures between 750 and 800°C (samples A800, H750 and H800) present almost the same crystallite sizes, but they are twice smaller than the corresponding to the powder sintered at 900°C (sample A900). The crystallite sizes of samples H800 and A900 were also calculated applying the Rietveld method, using an isotropic size and strain broadening model [12], and the obtained values were comparable to those obtained by Scherrer formula.
Transmission electron microscope (TEM) observations (see Figures 1b and 1c) not only revealed that grain sizes of powders prepared by acetate method are usually larger than those prepared by HMTA method; but also that sample H800 presents a more homogeneous size distribution than sample A900. Accordingly, powders prepared by HMTA route present larger surface area than those synthesized by acetate method (see Table 1).
X-ray diffraction patterns of LSCF/CGO/LSCF cells only show reflections corresponding to LSCF and $Ce_{0,1}Gd_{0,9}O_{2-\delta}$ phases, suggesting that there was no chemical reaction between cathode and electrolyte (see Figure 2a). Films crystallite sizes are similar than those of powder samples prepared with analogous conditions (see Tables 1 and 2), indicating that the same synthesis mechanism is present in both. No changes in crystallite size were founded after impedance measurements within experimental errors.
Figures 2b and 2c show Scanning Electron Microscopy (SEM) images from cathodes prepared with Acetate and HMTA methods. Surfaces images were taken before impedance measurements and cross-sectional images after them. Non significant increase of particle size was found after impedance measurement. Cathodes prepared with HMTA powders have approximately 30% smaller particle sizes than those of cathodes prepared by Acetate method (see Table 2). Additionally, the cathode porous distribution obtained is different for each method (see Figures 2b and c).

ASR average values of all samples prepared with the same method are plotted in Figure 3 (ASR differences up to ±30% were found, represented within the error bars). Murray et al [13] also found variations in LSCF spin coated samples, but up to a factor of 3. These variations may be due to ink ageing, or inherent to the spin coating deposition. Regardless, data dispersion is not relevant when referred to the difference among other ASR reported values also shown in Figure 3. For example, our samples ASR values are more than two orders of magnitude lower than those corresponding to a cathode with identical composition also prepared by Acetate method but sintered at 1000°C and deposited by spraying [5,14]. Furthermore, our ASR values are the lowest at low temperatures (400 – 500 ºC), being considerably below those reported for cathodes with similar composition and morphology prepared by other methods, and are even lower than the best known cathodes for IT-SOFC like BSFC (see Table 2).

Our cathodes present a slope change around 550 – 600 ºC, but the ASR values were almost reproduced in the cooling cycle. EIS carried out at different oxygen partial pressures suggests that this slope change is due to a difference in the oxygen reduction reaction mechanism [19].

Several authors have pointed out that cathode microstructure (i.e. particle size, pore size, tortuosity, etc.) strongly influences the ASR cathode values [2,4,7,20]. Accordingly, the excellent performance of our cathodes could be mainly explained by their optimal microstructure. The small grain size achieved by the synthesis methods would not only minimize the superficial related oxygen reduction limiting steps but also would improve the contact area at electrode/electrolyte-interface when combined with the spin coating technique.

The low ASR values obtained are very promising to open the 400-500°C temperature range to use IT-SOFC. However, the testing of these cathodes in a full electrolyte- or anode-support cell is planned in order to evaluate their performance under actual operation conditions.

4. Conclusions

LSCF cathodes with excellent electrochemical performance were prepared by Acetate and the novel HMTA routes. The latter allows obtaining LSCF single phase at temperatures as low as 800 °C and nanocrystalline grains. Our results reveal that IT-SOFC cathode performance strongly depends on microstructure and that ASR can vary more than two orders of magnitude for the *identical composition* and different morphologies, reaching values as low as 0.05 Ωcm^2 at 600˚C and 0.4 Ωcm^2 at 450˚C using the novel chemical route. Consequently, it is possible to open the 400-500°C temperature range to use IT-SOFC diminishing the problems associated with long-term use degradation.

Acknowledgments

Liliana Mogni, Nicolás Grunbaum and Liliana Morales are acknowledged for useful discussions. The authors thank to Ernesto Scerbo and Carlos Cotaro for SEM observations and Gustavo Pastrana for BET analysis at CAB-CNEA. This work was funded by UNCuyo, CONICET and ANPCyT.

References

[1] B. Steele, A. Heinzel, Nature 414 (2001) 345.

[2] E. Ivers-Tiffée, A. Weber, D. Herbstritt, J. European Ceramic Society 21 (2001) 1805.

[3] J. S. Yoon, R. Araujo, N. Grunbaumb, L. Baqué, A. Serquis, A. Caneiro, X. G. Zhang,

H. Y. Wang, Applied Surface Science 254 (2007) 266.

[4] M. Sase, J. Suzuki, K. Yashiro, T. Otake, A. Kaimai, T. Kawada, J. Mizusaki, H. Yugami, Solid State Ionics 177 (2006) 1961.

[5] L. Baqué, A. Serquis, N. Grunbaum, F. Prado, A. Caneiro, Mater. Res. Soc. Symp. Proc. 928 (2006) 181.

[6] M. Bellino, J. Sacanell, D. Lamas, A. Leyva, N. Walsöe de Reca, J. Am. Chem. Soc. 129 (2007) 3066.

[7] I. Kivi, P. Möller, H. Kurig, S. Kallip, G. Nurk, E. Lust, Electrochemistry Comm. 10 (2008) 1455.

[8] J. Serra, H.-P. Buchkremer, Journal of Power Sources 172 (2007) 768.

[9] Y. Xia, T. Armstrong, F. Prado, A. Manthiram, Solid State Ionics 130 (2000) 81.

[10] M. Gaudon, C. Laberty-Robert, F. Ansart, P. Stevens, A. Rousset, Solid State Sciences 5 (2003) 1377.

[11] C. Deportes, M. Duclot, P. Fabry, J. Fouletier, A. Hammou, M. Kleitz, E. Siebert, J. Souquet (Eds.), Electrochimie des Solides, PUG, 2004, 305.

[12] J. Rodriguez-Carvajal, *An introduction to the Program Full-Prof 2000*, July **2001**.

[13] E. Murray, M. Sever and S. Barnett, Solid State Ionics 148 (2002) 27.

[14] N. Grunbaum, L. Dessemond, J. Fouletier, F. Prado, A. Caneiro, Solid State Ionics 177 (2006) 907.

[15] F. Deganello, V. Esposito, M. Miyayama, E. Traversa, J. Electrochem. Society 154 (2007) A89.

[16] V. Dusastre, and J. Kilner, Solid State Ionics 126 (1999) 163.

[17] Z. Shao, S. Haile, Nature 431 (2004) 170.

[18] D. Beckel, U. Muecke, T. Gyger, G. Florey, A. Infortuna, L. Gauckler, Solid State Ionics 178 (2007) 407.

[19] L. Baqué, in preparation.

[20] M. Kuznecov, P. Otschik, P. Obenaus, K. Eichler, W. Schaffrath, Solid State Ionics, 157 (2003) 371.

Published in Electrochemistry Communications 10 (2008) 1905–1908 -
doi:10.1016/j.elecom.2008.10.010

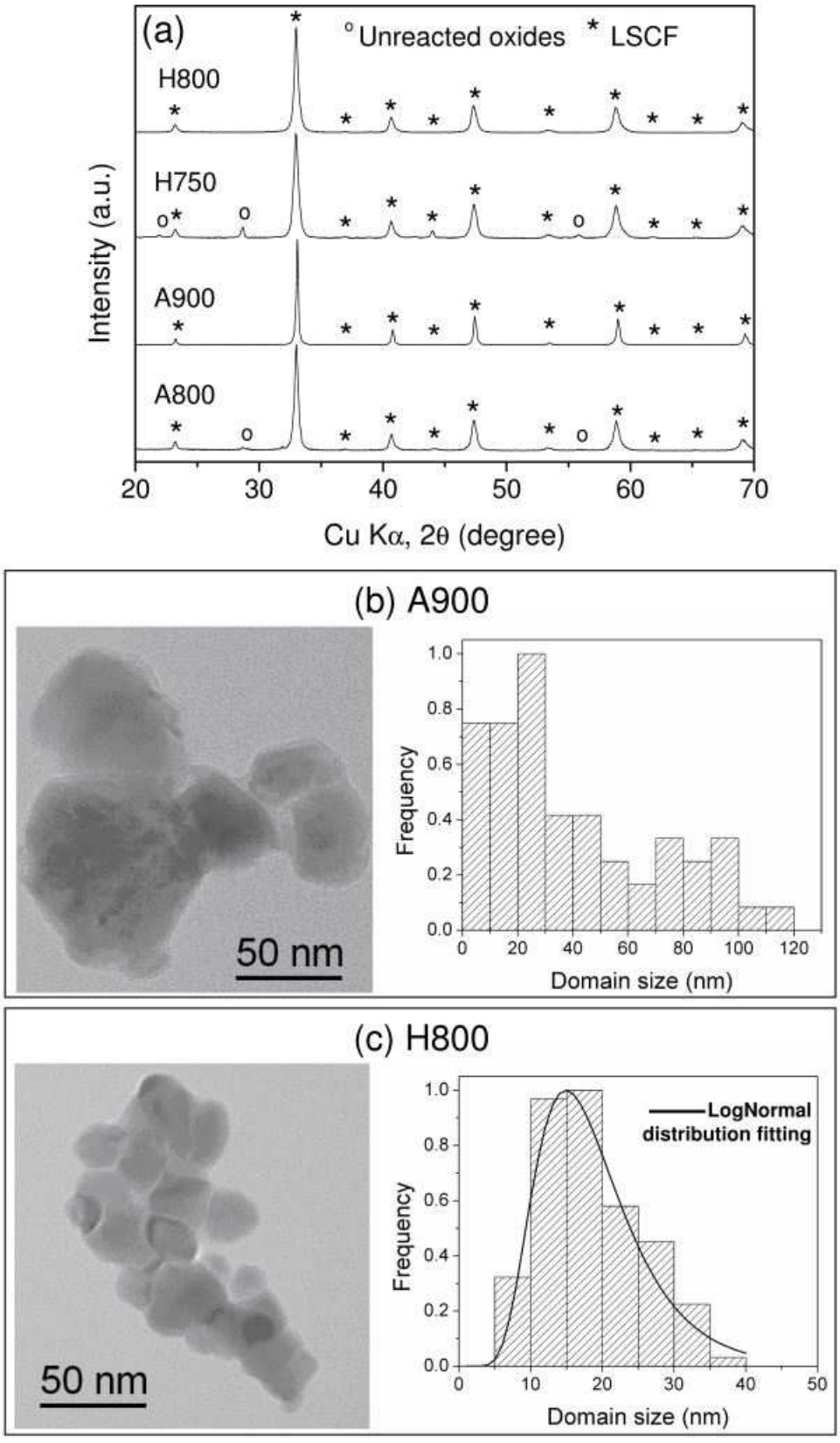

Figure 1. ***Powder samples characterization:*** **(a)** XRD data from samples listed in Table 1 **(b)**, **(c)** TEM images and size distributions from samples H800 and A900. The statistics were made over 70-100 crystalline domains using both high resolution and dark field images.

Published in Electrochemistry Communications 10 (2008) 1905–1908 -
doi:10.1016/j.elecom.2008.10.010

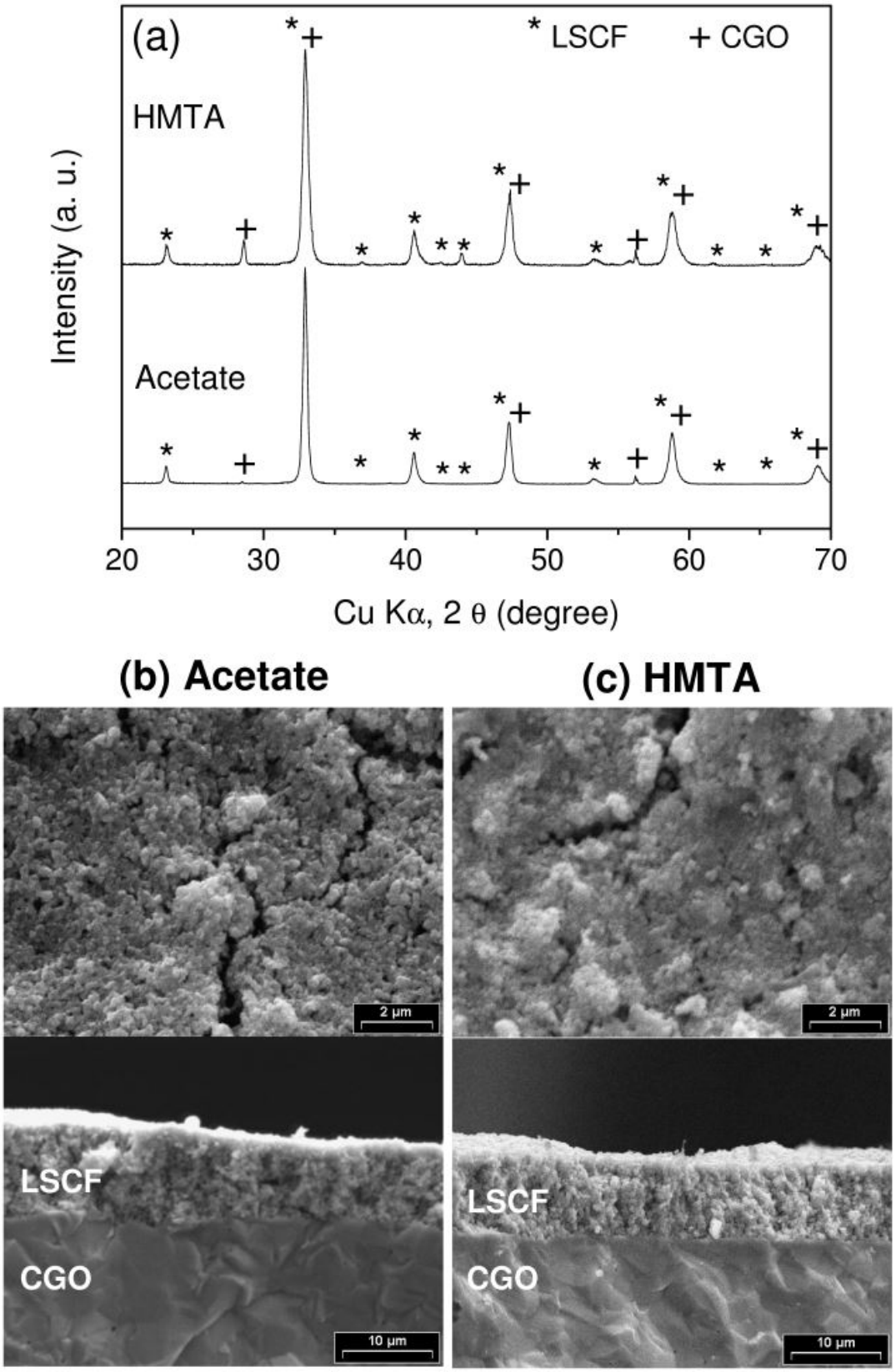

Figure 2. ***LSCF/CGO/LSCF cells characterization:*** **(a)** XRD data and **(b),(c)** SEM images of cathodes prepared by Acetate and HMTA. The upper and lower images display cell surfaces and cross-sectional morphologies, respectively.

Published in Electrochemistry Communications 10 (2008) 1905–1908 -
doi:10.1016/j.elecom.2008.10.010

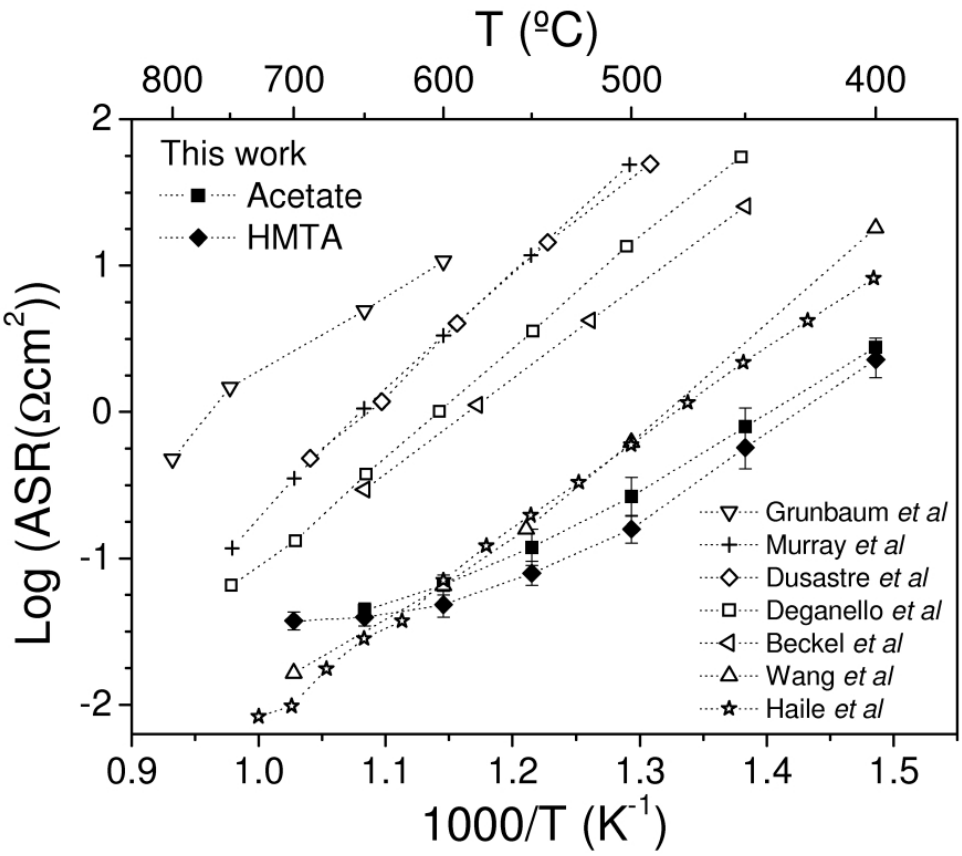

Figure 3. Arrhenius plot of our cathodes in comparison with other cathodes reported in literature (for references see **Table 2**). Dotted lines are guides to the eyes.

Sample	Preparation method	T_S (°C)	XRD size (nm)	Surface area (m^2/gr)
A800	Acetate	800	23 ± 4	8.3 ± 0.1
A900	Acetate	900	51 ± 8	4.15 ± 0.05
H750	HMTA	750	20 ± 3	12.35 ± 0.02
H800	HMTA	800	21 ± 3	10.5 ± 0.1

Table 1. Sintering temperature (Ts), crystallite size estimated from XRD data and surface area determined by BET.

Published in Electrochemistry Communications 10 (2008) 1905–1908 -
doi:10.1016/j.elecom.2008.10.010

Cathode	Electrolyte	T_{HT} (ºC)	Thickness (μm)	Particle size (nm)	Reference
$La_{0.4}Sr_{0.6}Co_{0.8}Fe_{0.2}O_{3-\delta}$ (Acetate method)	$Ce_{0.9}Gd_{0.1}O_{2-\delta}$	900	11 ± 3	180 ± 40 [a] (40 ± 10 [b])	This work
$La_{0.4}Sr_{0.6}Co_{0.8}Fe_{0.2}O_{3-\delta}$ (HMTA method)	$Ce_{0.9}Gd_{0.1}O_{2-\delta}$	800	10 ± 2	130 ± 30 [a] (27 ± 3 [b])	This work
$La_{0.4}Sr_{0.6}Co_{0.8}Fe_{0.2}O_{3-\delta}$	$Ce_{0.9}Gd_{0.1}O_{2-\delta}$	1000	20	600	Grunbaum *et al* [5]
$La_{0.6}Sr_{0.4}Co_{0.95}Fe_{0.05}O_{3-\delta}$	$Ce_{0.8}Sm_{0.2}O_2$	900	[c]	150	Deganello *et al* [15]
$La_{0.4}Sr_{0.6}Co_{0.8}Fe_{0.2}O_{3-\delta}$	$Ce_{0.9}Gd_{0.1}O_{2-\delta}$	[d]	2	[c]	Yoon *et al* [3]
$La_{0.6}Sr_{0.4}Co_{0.2}Fe_{0.8}O_{3-\delta}$	$Ce_{0.9}Gd_{0.1}O_{2-\delta}$	800	10-15	[c]	Dusastre *et al* [16]
$La_{0.6}Sr_{0.4}Co_{0.2}Fe_{0.8}O_{3-\delta}$	YSZ	900	20	100-200	Murray *et al* [13]
$Ba_{0.5}Sr_{0.5}Co_{0.8}Fe_{0.2}O_{3-\delta}$	$Ce_{0.85}Sm_{0.15}O_2$	1000	20	[c]	Shao *et al* [17]
$Ba_{0.25}$ $La_{0.25}Sr_{0.5}Co_{0.8}Fe_{0.2}O_{3-\delta}$	$Ce_{0.8}Gd_{0.2}O_{2-\delta}$	650	0.6	35	Beckel *et al* [18]

Table 2. Cathode and electrolyte compositions, heat treatment temperature, thickness and particle size of cathodes shown in Figure 3.

[a] Particle size determined by SEM (these particles are agglomerates of several single crystalline grains)
[b] Crystallite size determined from XRD data
[c] Not reported
[d] PLD deposited at 100–500 °C.